A Naive Model for the Pomeron Structure Function from Diffractive Deep Inelastic Scattering

José Montanha

Instituto de Física Gleb Wataghin, Universidade Estadual de Campinas, Unicamp, 13083-970, Campinas, São Paulo, Brasil
e-mail: montanha@ifi.unicamp.br

Abstract

Deep inelastic electron-proton scattering has been a fundamental tool for the understanding of the partonic structure of hadrons. In recent years new experimental findings in deep inelastic scattering coming from DESY brought a new light into an important domain of hadronic physics, the diffractive interaction of hadrons, dominated by the exchange of a color singlet with the quantum numbers of the vacuum, known as pomeron. Due to its long distance nature, diffractive reactions reside outside the region of perturbative quantum chromodynamics applicability, and therefore lack a proper quantum field theory description. In this article, we present a naive phenomenological model that associates non-perturbative aspects of diffraction with the dynamics of QCD, to describe some experimental data from DESY and to built a simple partonic picture of the pomeron. From the model, we found that the pomeron structure function can be described as dominated by gluons.

1 Introduction

Hadrons are defined as the particles that experience the strong nuclear force. According to the standard theory of the strong interaction, quantum chromodynamics (QCD), hadrons are composite states of more fundamental particles, quarks and gluons. Quarks are electrically charged, massive fermions responsible for the hadron quantum numbers, while gluons are electrically neutral, massless gauge field bosons, responsible for transmitting the strong force between the quarks.

Both quarks and gluons, collectively known as partons, carry the charge of the strong force, known as the color charge. Since color charge does not manifest itself in the physical world, all hadrons have to be neutral color states of quarks and gluons, or color singlets.

A high energy hadron-hadron collision is a very complex process involving the interaction of quarks and gluons of both hadrons. The perturbative approach to QCD, that is applied to describe such processes, relies on the existence of a hard energy scale in the interaction, which means that the hadrons have to come close enough of each other during the collision to allow their partons to interact individually as free particles. Such hadronic reactions are called *hard scattering*.

The need of a hard scale in the reaction comes from the fundamental parameter of QCD, the running coupling constant α_s, that gives the strength of the interaction between partons. Its value is a function of the distance over which the parton has been probed, since the highest the probe momentum the shorter the distances it can resolve. In the leading-logarithm (lowest order correction) approximation, the QCD running coupling constant reads [1]

$$\alpha_s(q^2) = \frac{\alpha_s(q_o^2)}{1 + B\,\alpha_s(q_o^2)\,ln\frac{q^2}{q_o^2}} = \frac{1}{B\,ln\frac{q^2}{\Lambda^2}}, \qquad (1)$$

where q is the four-momentum transfer in the interaction, q_o is a starting value of q, for which $\alpha_s(q_o^2)$ is small enough to justify a perturbation expansion, $\Lambda^2 = q_o^2 \exp\left[-1/B\alpha_s(q_o^2)\right]$ and $B = (33 - 2f)/12\pi$, where f is the number of quark flavors. Therefore, for a number of quark flavors $f \leq 16$, it follows that $\alpha_s(q^2)$ decreases as q^2 increases (note that in the current standard model of the strong interaction, the number of quark flavors[1] is 6, safely below the upper limit of 16). As $q^2 \to \infty$, we have that $\alpha_s(q^2) \to 0$ and the quarks in the hadron behave as free particles. This is called the *asymptotic freedom* regime. If, however, q^2 is much lower than q_0^2, the strong coupling constant $\alpha_s(q^2)$ becomes large, and the perturbative approach of QCD becomes meaningless. This regime is related with the *confinement* of the partons in the hadron, meaning that at large distances (low four-momentum transfer squared q^2) the quarks cannot be seen as free particles anymore. In that regime, the hadronic reaction turns to be a intricate interaction between the partons, with complex color radiation patterns, that make the calculations unaccessible.

Most of the hadronic scattering processes are *soft*, which means that they are long distance interactions that lack a hard scale to allow perturbative QCD to be applied. Among the *soft scattering* processes, there is a class of hadronic reactions named *diffractive scattering*, which has an important hole in high energy collisions. At Fermilab's Tevatron collider energy ($1800\,GeV$ in the collision center of mass system), approximately 40% of the total antiproton-proton ($\bar{p}p$) cross section comes from soft diffractive scattering.

[1] The quark flavors are *up (u), down (d), strange (s), charm (c), botton (b)* and *top (t)*

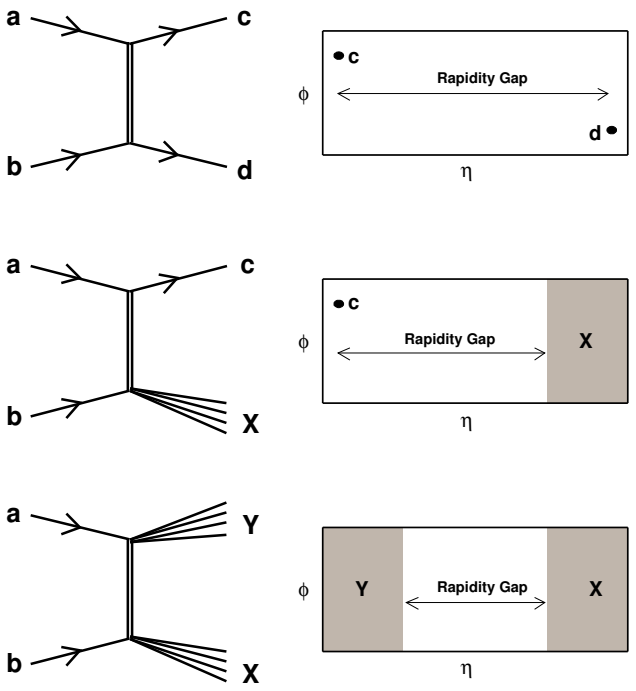

Figure 1: Soft diffraction reactions between hadrons a and b. From top to bottom: Elastic scattering, single and double diffraction. On the right, the respective plot of each interaction showing the distribution of particles in the final state. For more details, see Section 6.

The distinctive experimental characteristic of diffractive interactions is the scattering and/or production of particles in the forward (small angle) direction, close to the incoming particle beam. Therefore, there is a large angular region (relative to the incoming beam) with no particles detected, or, on the language of experimental particle physics, a large rapidity gap (see Section 6 for the definition of rapidity and rapidity gap).

From a theoretical point of view, since there is no change of quantum numbers between the initial and final state of the interaction, hadronic diffraction means the exchange of the vacuum quantum numbers between the particles (see Table 1. For more details, see ref. [2]).

The name *diffraction* comes from a optical interpretation of these interactions, where the incoming high energy proton wave function can be thought as been diffracted by the target nucleon, that acts like an absorbing disc [3].

Figure 1 illustrates the most important hadronic diffraction processes: elastic scattering, single and double diffraction[2].

Elastic scattering corresponds to the process where the initial state particles (a and b) and the final state particles (c and d) are the same, so that we actually have the reaction $a\,b \rightarrow a\,b$. In the reaction, there is no change in the quantum numbers when it goes from the initial to the final state, therefore the reaction exchange the quantum numbers of the vacuum. Both particles are scattered in opposite directions to each other, leaving a rapidity gap between them, and the highest the energy of the collision, the largest the rapidity gap. So, at high energies, hadronic elastic scattering totally fulfill the requirements of a diffractive event. In fact, elastic scattering is a very important channel in hadron-hadron diffractive interactions, since the Optical Theorem [4] allows to establish a relation between the total cross section of a reaction and the imaginary part of the forward elastic scattering amplitude of the same reaction,

$$\sigma(s) = \frac{4\pi}{s} ImF(s, t = 0), \tag{2}$$

where the variables s and t are the square of the center of mass energy and the four-momentum transfer in the reaction (they are discussed in more detail in Section 6). The connection between experiment and theory comes through the differential elastic cross section, written in terms of the elastic scattering amplitude $F(s, t)$ as

$$\frac{d\sigma_{el}}{dt} = \frac{\pi}{s^2} |F(s, t)|^2 \,. \tag{3}$$

Single diffraction corresponds to a scattering where one of the initial state particles, a or b, survives the collision, being observed in the final state as particle c, in a similar fashion as in the elastic scattering. The other incoming particle is excited into a higher energy state (a resonance), which decays in a state X of particles with total mass M_X, keeping the same quantum numbers of the original one. The process $a\,b \rightarrow c\,X$ is inelastic, since a fraction of the initial state energy is used in the excitation of one of the incoming hadrons. It however fulfill the conditions to classify itself as diffractive, since the quantum numbers of the initial state do not change in the reaction, and a large rapidity gap is observed in the final state. Note that nowadays, in high energy physics, the word *diffraction* is usually used to refer specifically to inelastic single diffraction.

In double diffraction, both initial state particles, a and b, fragment themselves, producing systems X and Y of particles with mass M_X and M_Y in the final state, $a\,b \rightarrow X\,Y$. This reaction can still be classified as diffractive when the final states X and Y are identified as fragments of the particles a and b, with same quantum numbers as these particles and a large rapidity gap between them.

Since these hadronic soft interactions cannot be described by the methods of perturbative quantum chromodynamics (pQCD), they lack a more fundamental understanding in terms of quarks and gluons. In fact, the description of the

[2]The kinematics for hadronic interactions is described in Section 6

bulk of soft hadronic scattering relies on a plethora of phenomenological models [5], and a set of fundamental theorems established in quantum mechanics [6], like the optical theorem above, Eq. (2).

A very successful framework for the description of high energy soft scattering comes from a complex angular momentum theory, known as Regge Pole Theory [2]. It starts from an expansion of the scattering amplitude in partial waves, where it is assumed that the partial wave amplitude $f(j,t)$ is dominated by a finite number of isolated, simple, moving poles located in the complex angular momentum plane j at some value $\alpha(t)$,

$$f(j,t) = \frac{\beta(j)}{(j-\alpha(t))}. \tag{4}$$

The parameter $\alpha(t)$ is known as a Regge trajectory, and it is determined phenomenologically from plots of mass squared versus angular momentum of mesons. A family of meson resonances (a group of mesons with same isospin, parity and charge conjugation quantum numbers[3]) differ only by the mass and angular momentum of their constituents, and for a meson of mass squared m^2, its angular momentum is $j = \alpha(t = m^2)$. From such plots, known as Chew-Frautschi plots, it is found that the trajectory $\alpha(t)$ is a linear function of t, written as $\alpha(t) = \alpha_0 + \alpha' t$, where α_0 is the intercept of the trajectory, and α' is its slope. Every family of meson resonances (like f_2, ω, ρ, etc) has an associated trajectory, and a given hadron-hadron scattering can only exchange trajectories associated with meson families with the correct quantum numbers for that reaction [5].

An important result coming from the Regge Pole approach of hadron interactions is that the elastic scattering amplitude $F(s,t)$, in the limit $s \to \infty$, with constant t, is given by

$$F(s,t) = \tau(t)\beta(t)(\frac{s}{s_o})^{\alpha(t)}, \tag{5}$$

where $\beta(t)$ is a residue function, s_o is an arbitrary soft scale (usually $s_o = 1\,GeV^2$), and $\tau(t)$ is given by

$$\tau(t) = \frac{(1+\tau\exp i\pi\alpha(t))}{\sin\pi\alpha(t)}. \tag{6}$$

Here, τ is known as signature, and it is $+1$ for even angular momentum trajectories, and -1 for odd angular momentum trajectories.

Using Eq. (5) at $t = 0$ in Eq. (2), we have a phenomenological parameterization for the energy dependence of the total $\bar{p}p$ cross section

$$\sigma_{tot}^{\bar{p}p}(s) = \sum_i A_i\,(s/s_0)^{\alpha(0)-1}, \tag{7}$$

where A_i is an energy independent parameter associated with the trajectory i, and we have to sum over all possible Regge trajectories that can be exchanged in a $\bar{p}p$ collision [8]. Since the intercept $\alpha(0)$, for all known meson families, has approximately the same value, $\alpha(0) \approx 0.5$ [2], the total $\bar{p}p$ cross section is supposed to fall as $\sigma_{tot} \to s^{-0.5}$ when $s \to \infty$.

Experimentally, all hadron-proton cross sections rise with increasing s [9] and, to account for that experimental fact, one new trajectory was introduced, with an intercept $\alpha(0) = 1+\epsilon$ (with $\epsilon > 0$), so that as $s \to \infty$, $\sigma_{tot} \to s^{\epsilon}$. This new, phenomenological, object received the name *pomeron* (simbol $I\!P$) in honor to the Russian physicist I. Y. Pomeranchuk, one of the pioneers in the field of hadronic diffraction. According to the present theoretical understanding, the pomeron is the object exchanged in a diffractive reaction, being identified as the color singlet that carries the quantum numbers of the vacuum, and with the highest Regge trajectory intercept. However, up to now, no resonance or bound state was identified with its trajectory. Table 1 present the quantum numbers associated with the pomeron.

Table 1: Pomeron (vacuum) quantum numbers: Q - charge; I - isospin; S - strangeness; B - baryon quantum number; P - parity; C - charge conjugation; τ - signature [2].

Q	*I*	*S*	*B*	*P*	*C*	τ
0	*0*	*0*	*0*	*+1*	*+1*	*+1*

In 1985 G. Ingelman and P. Schlein [10] suggested that if the pomeron has a partonic structure, it would be able to perform a hard scattering. They treated the pomeron as a particle, and pictured a hard diffractive interaction as a two step process. First the pomeron would be emitted by one of the hadrons, as in a soft process. Second, the partons of the pomeron would be scattered by the partons of the second hadron, producing a hard scattering. In the end, the process would be similar to the single diffraction of Figure 1, but the final state X would be composed of jets of particles, a signature of a hard scattering.

In the Ingelman-Schlein model, the differential cross section for the production of jets, $\frac{d^2\sigma_{jj}}{dtdM_X^2}$, is given by the product of the probability of each step;

$$\frac{d^2\sigma_{jj}}{dtdM_X^2} = \frac{d^2\sigma_{sd}}{dtdM_X^2}\,\frac{\sigma_{pIP\to jj}}{\sigma_{pIP\to X}}, \tag{8}$$

[3]For a definition of isospin, parity and charge conjugation, see [7]

where $\sigma_{pIP\to jj}$ is the cross section for a hard pomeron-proton scattering, $\sigma_{pIP\to X}$ is the pomeron-proton total cross section, and $d^2\sigma_{sd}/dtdM_X^2$ is the differential single diffraction cross section. The last two terms are well known from soft hadronic phenomenology, and can be combined to give the flux of the pomeron in the reaction,

$$g_{I\!P}(\xi) = \frac{1}{\sigma_{pIP\to X}} \frac{d^2\sigma_{sd}}{dtdM_X^2}. \qquad (9)$$

Such process, that is called *hard diffraction*, was observed, at CERN's Super antiproton-proton Sincrotron (S$\bar{p}p$S) Collider, (collision center of mass energy of $630\,GeV$) in 1988, by the UA8 Collaboration [11], and it showed that the pomeron could be experimentally studied as a QCD object.

However, since a hadron-hadron collision is a very complicated process involving parton-parton interactions from both hadrons, the best experimental, as well as theoretical, way to study the inner structure of the hadrons is through electron-proton deep inelastic scattering. Therefore, it was only with the observation of hard diffraction in electron-proton (e^-p) reactions in the 90's that a phenomenological program to describe the pomeron as an object of QCD took off [12].

In section 2 we briefly review some of the ideas related with deep inelastic scattering and diffractive deep inelastic scattering. In section 3 we introduce our model for the description of the diffractive deep inelastic scattering data in terms of a pomeron exchange, and in section 4 we discuss the results and present the conclusions.

2 Diffractive Deep Inelastic Scattering

Deep inelastic e^-p scattering (DIS) has been a fundamental tool for the understanding of the internal structure of the proton in terms of its partonic constituents, and has provided the experimental proof that QCD is the correct theory of the strong force [7].

The advent of the Hadron-Electron Ring Accelerator (HERA), in the Deutsches Elektronen-Synchrotron (DESY) at Hamburg, Germany, in 1992, opened new grounds for testing QCD. The high energy collision between $27.5\,GeV$ electrons (or positrons) and $920\,GeV$ protons, allowed the experimentalists to explore deep into the structure of the proton, covering a resolution interval from $1fm$ to $10^{-5}fm$, improving considerably the knowledge about the dynamics of proton's structure function.

Maybe the most significant result obtained at DESY's HERA collider was the discovery, by the H1 and ZEUS collaborations [13, 14], of deep inelastic scattering events where, besides the electron, also the proton survives the interaction, producing a large rapidity gap signal. Such events exhibit mass distributions whose shape resemble very much those observed in hadron-hadron diffraction experiments, and therefore the process was named *diffractive deep inelastic scattering* (DDIS).

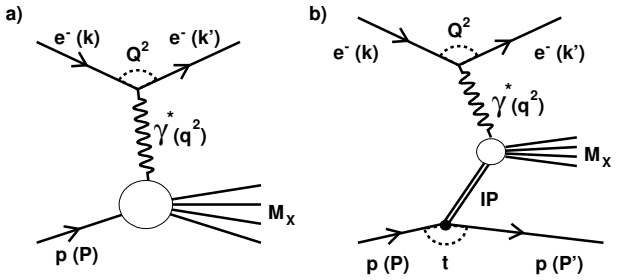

Figure 2: Deep inelastic e^-p scattering diagrams, with the relevant kinematic variables; a) conventional DIS process and b) diffractive DIS, with the incoming proton exchanging a pomeron $I\!P$ and surviving in the final state.

In a deep inelastic scattering (DIS) process, $e^-p \to e^-X$, a high energy electron (or positron) of four-momentum k interacts with a proton of four-momentum P through the emission of a photon of four-momentum q. As long as the photon has high enough q^2, it can resolve the internal partonic structure of the proton, interacting with its charged partons through a hard scattering which breaks up the proton. Therefore, in the e^-p DIS, the fundamental interaction takes place between the probing photon and a proton's charged parton that the photon strikes, producing a γ^*q scattering. Experimentally, in this inclusive reaction only the outgoing electron is detected in the final state (fig. 2a).

The usual variables employed to describe e^-p DIS are depicted in Figure 2a. One can define the squared energy in the e^-p center of mass system (cms) in terms of the four-momenta P and k, referring respectively to the incoming proton and electron (or positron), as

$$s \;=\; (P+k)^2 \qquad (10)$$

and the squared energy in the γ^*p cms as

$$W^2 \;=\; (P+q)^2. \qquad (11)$$

The photon four-momentum squared q^2, its virtuality Q^2, the Bjorken x and the variable y are given by

$$q^2 \;=\; -Q^2 = (k-k')^2; \qquad (12)$$

$$x \;=\; \frac{Q^2}{2\,P\cdot q} = \frac{Q^2}{W^2+Q^2-m_p^2}; \qquad (13)$$

$$y \;=\; \frac{P\cdot q}{P\cdot k}. \qquad (14)$$

The variable x represents the fraction of the proton's momentum that is carried by a struck parton in the proton, and

y is the fraction of the total $e^- p$ cms energy that goes into the $\gamma^* p$ reaction, or the inelasticity of the electron. If we ignore the proton mass, relative to the other variables, in the equations above, we have the following relations among these variables:

$$Q^2 = x\ y\ s \tag{15}$$

and

$$W^2 = Q^2\ \frac{(1-x)}{x} \simeq \frac{Q^2}{x}, \tag{16}$$

being that $x << 1$ has been assumed in the latter expression.

For the case presented in Figure 2b, where a proton with four-momentum P' is detected in the final state, we can also define the variables

$$t = (P - P')^2, \tag{17}$$

$$\xi = \frac{Q^2 + M_X^2 - t}{Q^2 + W^2}, \tag{18}$$

$$\beta = \frac{Q^2}{Q^2 + M_X^2 - t} = \frac{x}{\xi}, \tag{19}$$

the variables t and ξ have the same meaning as in the hadronic case (see section 6), where ξ is the lost fraction of the proton's momentum in the reaction, which is carried by the pomeron. Since x represents the fraction of the proton's momentum carried by a struck parton, and since the pomeron carries the fraction ξ of the momentum of the proton, then the β variable represents the fraction of momentum carried by a struck parton in the pomeron.

In the case of diffractive events, the DDIS cross section is often expressed in terms of the β and ξ variables,

$$\frac{d^3\sigma}{d\beta\ dQ^2\ d\xi} = \frac{4\pi\ \alpha_{em}^2}{\beta\ Q^4}\left[1 - y + \frac{y^2}{2(1+R)}\right] \times\ F_2^{D(3)}(\xi, \beta, Q^2). \tag{20}$$

Here $R = \sigma_L/\sigma_T$ is the ratio between the cross sections for longitudinally and transversely polarized virtual photons. Under certain conditions, it is possible to assume $R \approx 0$ and thus the experimental behavior of the cross section (20) is expressed in terms of the structure function $F_2^{D(3)}(\xi, \beta, Q^2)$ [15].

The structure function is a parameter that provides the connection between the observable cross section and the internal constituents of the hadron being probed by the photon, since it is written in terms of parton distributions in the hadron. Thus, the diffractive structure function provides information about the behavior of partonic content of whatever is being probed in a DDIS. However, the connection between the observable structure function and the parton distributions in the pomeron is totally model dependent, and in the next section we explore a simple model of the pomeron to show how to get some insights about its quark and gluon content.

3 Model and Parameters

For the present study we have used the diffractive structure function data $F_2^D(3)$ obtained by the Zeus Collaboration [14], to test a simple model which assumes that such structure function can be described by the product of two terms; the probability of emission of a pomeron by the proton, and the pomeron structure function itself, as probed by the virtual photon. The model follows a close analogy with the Ingelman-Schlein model for hadronic hard diffractive scattering, and the diffractive structure function is written as

$$F_2^{D(3)}(\xi, \beta, Q^2) = g_{I\!P}(\xi)\ F_2^{I\!P}(\beta, Q^2). \tag{21}$$

Here, the function $g_{I\!P}(\xi)$ represent the pomeron flux factor, while $F_2^{I\!P}(\beta, Q^2)$ is the pomeron structure function.

Therefore, the model assumes a factorization between the soft hadronic vertex of Figure 2b, responsible for the emission of a pomeron carrying the fraction ξ of the incoming proton's momentum, and the hard $\gamma^* I\!P$ scattering. With that hypothesis, most of the parameters related with the pomeron flux factor can be taken from soft hadronic phenomenology. The pomeron structure function could then be extracted directly from fits to the data. However, we are going to apply here a parameterization already obtained in a previous analysis of a larger set of DIS data, covering a broader kinematical interval, where the pomeron were one of several possible exchanges taking place [16].

We take the pomeron flux from Regge phenomenology of hadronic soft diffraction [17], where it is written as

$$g_{I\!P}(\xi) = \xi^{1-2\alpha_{I\!P}^0} \int_{|t_{min}|}^{|t_{max}|} e^{-(\alpha_{I\!P}' ln\xi)\ t}\ F_1^2(t)\ dt \tag{22}$$

where $|t_{min}|$ and $|t_{max}|$ are the minimum and maximum absolute t values of the t-integrated experimental data. In this expression, the parameters $\alpha_{I\!P}^0$ and $\alpha_{I\!P}'$ are, respectively, the intercept and slope of the pomeron linear trajectory, that is

$$\alpha_{I\!P}(t) = \alpha_{I\!P}^0 + \alpha_{I\!P}'\ t, \tag{23}$$

and $F_1(t)$ in Eq. (22) is the Dirac form factor given by

$$F_1(t) = \frac{4m_p^2 - 0.28t}{4m_p^2 - t}\left(\frac{1}{1 - t/0.71}\right)^2. \tag{24}$$

where m_p is the mass of the proton. We take their values from [16] as $\alpha_{I\!P} = 1.2$ and $\alpha_{I\!P}' = 0.25\, GeV^2$.

For the pomeron structure function, as mentioned before, we choose a functional form based on the a previous phenomenological analysis of leading particle structure function data in DIS at HERA [16]. The quark flavor singlet distribution $\beta S_q(\beta, Q^2) = u + \bar{u} + d + \bar{d} + s + \bar{s}$ and the gluon distribution $\beta G(\beta, Q^2)$ are parameterized in terms of the coefficients $C_j^{(S)}$ and $C_j^{(G)}$, according to:

$$\beta S(\beta, Q^2 = Q_0^2) = \left[\sum_{j=1}^{n} C_j^{(S)} \cdot P_j(2\beta - 1)\right]^2 \times exp(\frac{a}{\beta - 1}) \quad (25)$$

$$\beta G(\beta, Q^2 = Q_0^2) = \left[\sum_{j=1}^{n} C_j^{(G)} \cdot P_j(2\beta - 1)\right]^2 \times exp(\frac{a}{\beta - 1}). \quad (26)$$

where $P_j(\zeta)$ is the j^{th} member in a set of Chebyshev polynomials, with $P_1 = 1$, $P_2 = \zeta$ and $P_{j+1}(\zeta) = 2\zeta P_j(\zeta) - P_{j-1}(\zeta)$. We have summed these terms up to $n = 3$ and set our hard scale $Q_0 = 2\,GeV^2$.

Since it is not possible to totally separate the pomeron structure function from its flux factor, the parameters $C_j^{(S)}$ above also set the overall normalization of the pomeron contribution. Their values are given in Table 3. The gluon and quark distributions above are evolved from $Q_0^2 = 2\,GeV^2$ up to the highest Q^2 of the Zeus data, in leading order (LO) and next-to-leading order (NLO) through the Altarelli-Parisi equation [18], that is written as

$$\frac{dS(\beta, Q2)}{d\ \ln Q^2} = \frac{\alpha_s}{2\pi}\int_\beta^1 \frac{dz}{z} [S(z, Q^2)P_{qq}(\frac{\beta}{z}) + G(z, Q^2)P_{qg}(\frac{\beta}{z})],$$

$$\frac{dG(\beta, Q2)}{d\ \ln Q^2} = \frac{\alpha_s}{2\pi}\int_\beta^1 \frac{dz}{z} [S(z, Q^2)P_{gq}(\frac{\beta}{z}) + G(z, Q^2)P_{gg}(\frac{\beta}{z})], \quad (27)$$

where P_{qq}, P_{qg}, P_{gq} and P_{gg} are the splitting functions that give the probability of a quark or gluon to open, respectively, a quark-quark, a quark-gluon, a gluon-quark or a gluon-gluon pair [1].

Table 2: Values of the pomeron's quark and gluon parton distribution functions, Eq. (25) and Eq. (26), taken from ref. [16].

Parameters	*Leading Order*	*Next to Leading Order*
$C_1^{(S)}$	0.111 ± 0.031	0.116 ± 0.017
$C_2^{(S)}$	0.076 ± 0.034	0.169 ± 0.029
$C_3^{(S)}$	0.156 ± 0.034	0.181 ± 0.035
$C_1^{(G)}$	1.110 ± 0.056	0.710 ± 0.052
$C_2^{(G)}$	0.817 ± 0.071	1.350 ± 0.053
$C_3^{(G)}$	0.284 ± 0.097	0.633 ± 0.168
a	0.001	

The final pomeron structure function is written in terms of the singlet quark distribution as

$$F_2^{I\!P}(\beta, Q^2) = < e^2 > (u + \bar{u} + d + \bar{d} + s + \bar{s}) = < e^2 > S_q(\beta, Q^2), \quad (28)$$

where $< e^2 >$ is the average charge of the distribution and, for three flavors (u, d and s), $< e^2 >= 2/9$. The gluon distribution is not included in the structure function because the virtual photon couples only with charged particles, therefore it can only directly measure the quark distribution. The role of the gluon distribution lies in the dynamical evolution of the distribution, as prescribed by the Altarelli-Parisi Eq. (27).

4 Results and Conclusions

The result of our naive model for the diffractive structure function, $F_2^{D(3)}(\xi, \beta, Q^2)$, as the factorised product of the pomeron flux factor times the pomeron structure function, Eq. (21), is tested against the Zeus Collaboration data [14], as shown in Figure 4. In the figure, the diffractive structure function data is plotted against ξ, for several fixed values of β and Q^2.

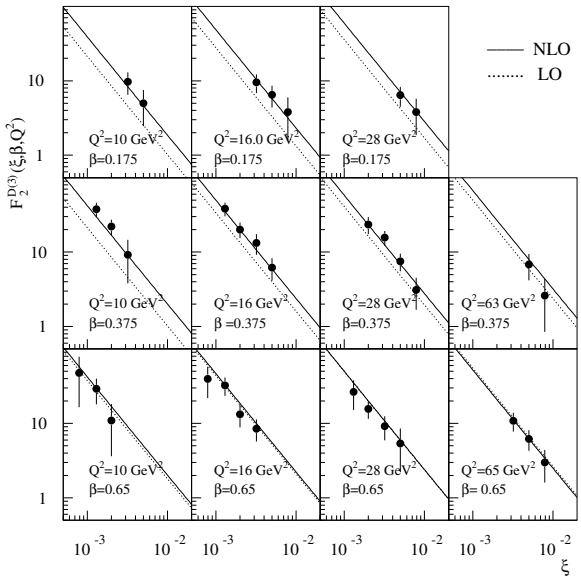

Figure 3: Diffractive structure function data $F_2^{D(3)}$ from Zeus Collab. [14], together with the results for the pomeron structure function extracted from NLO (solid line) and LO (dotted line) parameterizations for the parton distributions.

The plots of Figure 4 show that the data follows the ξ behavior from the pomeron flux, Eq. (22),

$$g_{I\!P}(\xi) \sim \xi^{-1.4}, \tag{29}$$

where we ignored here the very mild $\ln \xi$ contribution in the t-integral of Eq. (22), and substituted $\alpha^0_{I\!P} = 1.2$.

The ξ dependence of the diffractive structure function data corroborates the hypothesis of a factorization of $F_2^{D(3)}$ in a function related with the hadronic soft vertex and another related with the partonic interaction. Besides, the flux factor prediction of the ξ behavior, taken from hadron-hadron phenomenology, is in excellent agreement with the Zeus data behavior, since Eq. (29) correctly describes the slope behavior of those points, once the β and Q^2 values are kept constant, as shown in Figure 4. Since the ξ slope is governed by the choice of the trajectory's intercept in (22), such trajectory has to be higher than one to correctly describe the steeply fall of the data with ξ. This behavior alone is a signature of the pomeron exchange, and points towards the hypothesis that the nature of the phenomenon seems to be the same in both hadron-hadron and lepton-hadron interactions.

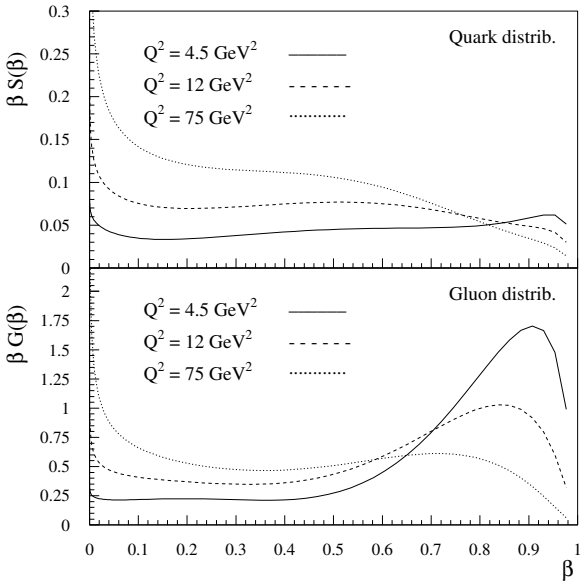

Figure 4: Parton distribution function versus the momentum fraction β of the parton, for quark and gluon distributions. The initial distribution, at $Q_o^2 = 2\,GeV^2$, is evolved for higher Q^2 using the Altareli-Parisi equation (27), in NLO.

To describe the β and Q^2 behavior we have to evolve the quark and gluon distribution functions, Eq. (25) and (26), using the Altareli-Parisi evolution equation, Eq. (27). The result in leading-logarithm order (LO, the lowest order correction for the running coupling constant $\alpha_s(Q^2)$) given in Eq. (1) does not describe correctly the data for low values of β and Q^2. With a more sensitive next-to-leading order (NLO) evolution of the parton distributions a very good agreement between model and data is achieved.

The behavior of the quark singlet and gluon distributions are show in Figure 4. Since, due to our model, the overall normalization of these distributions are connected with the normalization of the pomeron flux, we can only consider the relative values between the two distributions. The main result is that the pomeron structure function is mostly dominated by gluons, since that distribution surpass the quark one at any β. Also, since β is the momentum fraction of the pomeron carried by one of its partons, the gluon distribution function shows the gluons carrying a significant fraction of the pomeron's momentum at low Q^2 although, as Q^2 increases, the distribution flats down.

Concluding, diffractive deep inelastic scattering has proved to be an important experimental tool in the search of an unified picture of soft and hard regimes of hadron physics. We showed that by using a simple model, which borrows from both the Regge Pole Theory and the pQCD, it was possible to provide a satisfactory description of the diffractive structure function data from Zeus Collaboration. In the process, we were able to extract some information about the partonic structure of the pomeron, the object responsible for the hadronic diffraction. This kind of procedure only reflects the current state of affairs in the area, where experimental data are feeding up new phenomenological approaches, in the search of a final theory of hadronic interactions.

5 Acknowledgment

I would like to thank Fundação de Amparo à Pesquisa do Estado de São Paulo - FAPESP for providing the financial support to my research.

6 Appendix - Kinematics of Hadronic Diffractive Scattering

In the center of mass system (cms) of a high energy elastic reaction, Figure 6a, an anti-proton of four-momentum P_1 interacts with a proton of four-momentum P_2, both particles being scattered through an angle θ (relative to the incoming beam direction), leaving the interaction with four-momenta P_3 and P_4, respectively. For a single diffractive scattering reaction, Figure 6b, only one of the incoming hadrons is detected in the final state, with a four-momentum P_3, the other one breaking up in a system X of mass M_X that carries the same quantum numbers of the original particle P_2.

Since such processes are relativistic, the variables describing them have to be Lorentz invariants. For the exclusive (all final state particles detected) two body reaction from Figure 6a, the proper choices are the Mandelstam variables [7]

$$s = (P_1 + P_2)^2; \quad (30)$$

$$t = (P_1 - P_3)^2; \quad (31)$$

$$u = (P_1 - P_4)^2, \quad (32)$$

where s is the square of the center of mass energy of the collision, and t and u are the square of the four-momentum transferred in the reaction, in the forward and backward directions, respectively. These variables are connected by the relation

$$s + t + u = m_1^2 + m_2^2 + m_3^2 + m_4^2, \quad (33)$$

where the m_i's are the masses of the particles in the reaction. Therefore, in a two body reaction, like elastic scattering, there are only two independent variables, and the chosen ones are s and t.

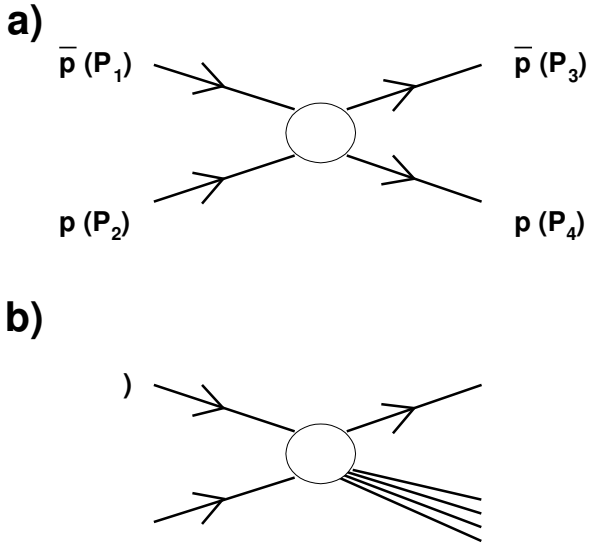

Figure 5: $\bar{p}p$ diffractive processes: a) elastic scattering and b) single diffractive dissociation.

Also in an elastic scattering, t is only a function of the center of mass scattering angle θ between the incoming and outgoing particles, since the absolute value of the three-momentum $\vec{k}$ of the particles does not change. In this case, the expression for t is

$$t = (P_1 - P_3)^2 = -4k^2 sin^2(\theta/2) \sim -k_T^2, \quad (34)$$

where k_T^2 is the transverse three-momentum squared of the elastically scattered particle. Note that, relative to the incoming particles direction, the three-momentum $\vec{k}$ of an outgoing particle can be separated into a transverse and a longitudinal component, $k = \sqrt{k_T^2 + k_L^2}$.

In an inclusive (only one kind of particle detected in the final state) reaction, the mass relation (33) reads

$$s + t + u = m_1^2 + m_2^2 + m_3^2 + M_X^2, \quad (35)$$

and now there are three independent variables, s, t and M_X^2, where M_X^2 is the squared mass of the system X, defined as

$$M_X^2 = (P_1 + P_2 - P_3)^2. \quad (36)$$

We also have that, in a single diffractive scattering, one of the incoming particles looses a fraction

$$\xi = \frac{(P_1 - P_3)}{P_1} \approx \frac{M_X^2}{s} \quad (37)$$

of its momentum, with $\xi \leq 0.15$ due to a coherence condition imposed over hadronic diffraction [19].

Another useful variable is the rapidity y, defined as

$$y = \frac{1}{2} \ln(\frac{E + k_L}{E - k_L}), \quad (38)$$

where E is the energy and k_L the longitudinal three-momentum of an observed particle in the final state. Since the relativistic energy of a particle of mass m and three-momentum $\vec{k}$ is given by $E^2 = m^2 + k^2$, where $k = \sqrt{k_L^2 + k_T^2}$, with k_T the transverse component of the three-momentum. At high energies (E and $k >> m^2$) and in the case where a particle is produced at high angles with the beam direction ($E >> k_L$), we would have $y \sim 0$. For a particle scattered in a direction very close to the beam ($k \sim \pm k_L$), we would have $y \to \pm y_{max}$. More precisely, the extreme values for the rapidity are

$$y_{max} = \pm \frac{1}{2} \ln \frac{s}{m^2}, \quad (39)$$

and therefore, at Tevatron, a $\bar{p}p$ elastic scattering provides a rapidity interval (or rapidity gap) between the outgoing proton and anti-proton of $\Delta y = \ln \frac{s}{m^2} \approx 15$.

A related variable, used more frequently by the experimentalists, is the pseudo-rapidity,

$$\eta = -\ln \tan \frac{\theta}{2}, \quad (40)$$

which relates a rapidity value with the scattering angle θ of the particle. For an elastically scattered proton at Tevatron ($s = 1800\, GeV$), $y \sim \eta \approx 7.5$, which corresponds to $\theta = 0.0011$ radians.

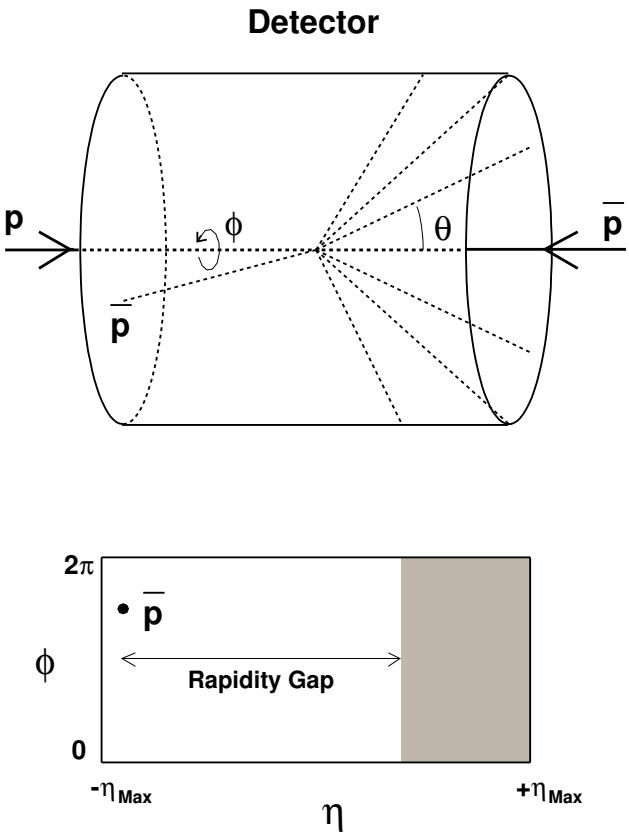

Figure 6: Geometrical representation of a $\bar{p}p$ diffractive processes: top) the detector has a cylindrical symmetry around the incoming particle beam bottom) The cylinder can be unfold to produce a 2D plot of the final state particle distribution in π, η phase space. For the $\bar{p}p$ collision illustrated, the antiproton survives the interaction, been scattered in a direction close to the incoming beam (high p_L, $\eta \sim \eta_{Max} \approx 7.5$). The proton dissociates in a state of particles that follow in the opposite direction, covering a large region of rapidity (the grey area on the plot).

Since diffractive reactions always produce large angular intervals devoid of particles (the already mentioned rapidity gaps), experimentally it is usual to associate diffraction with rapidity gaps. In the plot shown in Figure 6, the cylindric symmetry of a particle detector (top) was unfold in a rectangular plane (botton) the collision taking place at the center of the rectangle). The horizontal distances from the center are then associated with the rapidity (or zenithal) values of the produced particles, η, while the vertical distances are associated with the azimuthal angle ϕ. Is such plot the rapidity gap is the region of η, for any ϕ, with no particle detected.

References

[1] Donald H. Perkins, *Introduction to High Energy Physics* (chap. 8) Addison-Wesley Publishing, 1987; I. J. R. Aitchison and A. J. G. Hey, *Gauge Theories in Particle Physics* (chap. 9), IOP Publishing, Bristol, 1989.

[2] P. D. B. Collins, *An Introduction to Regge Theory and High Energy Physics*, Cambridge University Press, Cambridge, (1977);

[3] G. Alberi and G. Goggi, Phys. Rep. **74**, 1 (1981).

[4] C. Cohen-Tannoudji, *Quantum Mechanics*, (Vol. II, chap. VIII, complement B), Hermann, Paris, 1977.

[5] For a very padagogical review on Regge poles applied to high energy interactions see, for instance, J. M. Menon, *Introduction to Soft Diffraction: Some Results and Open Problems*, Proceedings of LISHEP 2002 - Session B: Advenced School on High Energy Physics, Rio de Janeiro, RJ, (2002). It will be soon available on the arXiv.org e-print archive.

[6] E. Predazzi, *Diffraction: Past, Present and Future*, Lecutures given at *Hadrons VI*, Florianopolis, Brasil, (1998), hep-ph/809454; V. Barone and E. Predazzi, *High Energy Particle Diffraction*, Springer Verlag, (2002).

[7] F. Halzen and A. D. Martin, *Quarks and Leptons: An Introductory Course in Modern Particle Physics*, John Wiley and Sons, 1984.

[8] R. J. M. Covolan, J. Montanha and K. Goulianos, Phys. Lett. **B389**, 176 (1996).

[9] A. Donnachie and P. V. Landshoff, Phys. Lett. **B296**, 227 (1992).

[10] G. Ingelman and P. Schlein, Phys. Lett. **B152**, 256 (1985).

[11] UA8 Collaboration, R. Bonino *et al.*, Phys. Lett. **B211**, 239 (1988).

[12] J. R. Forshaw and D. A. Ross, *Quantum Chromodynamics and the Pomeron*, Cambridge University Press, Cambridge, (1997).

[13] H1 Collaboration, T. Ahmed *et al.*, Phys. Lett. **B348**, 681 (1995).

[14] ZEUS Collaboration, M. Derrick *et al.*, Zeit. Phys. C **68**, 569 (1995).

[15] H1 Collaboration, C. Adloff *et al.*, Z. Phys. C **76**, 613 (1997).

[16] M. Batista, R. J. M. Covolan and J. Montanha, Phys. Rev. D **65**, 096006 (2002).

[17] K. Goulianos and J. Montanha, Phys. Rev. D **59**, 114017 (1999).

[18] G. Altareli and G. Parisi, Nucl. Phys. B **126** 297 (1977).

[19] K. Goulianos, Phys. Rep. **101**, 169 (1983).